Dual Ductility Mode Shear Walls: Concept and Behavior

M.S.R. Labafzadeh[1] and M. Ziyaeifar[2*]

1. PhD Student, Structural Engineering Research Center, International Institute of Earthquake Engineering and Seismology (IIEES), Tehran, Iran
2. Associate Professor, Structural Engineering Research Center, International Institute of Earthquake Engineering and Seismology (IIEES), Tehran, Iran,
* Corresponding Author; email: mansour@iiees.ac.ir

ABSTRACT

Shear walls are among the most common lateral load resisting systems, which are not recognized as efficient ductile structural components. Using any opening in the wall leads to disperse the inelastic behavior across the height of the wall and employ both flexural and shear ductility capacity of the system at the base and around the openings, respectively. Simple models were utilized to study the role of large openings in inelastic dynamic behavior of shear walls. Despite the constant total input energy, the amount of dissipated energy at the lower part of these walls is decreased to about two-third the value of ordinary shear walls. Consequently, the ductility demand diminished in the plastic hinge at the base and the required reinforcement detailing becomes simpler. However, marginal gains observed in the structural response such as base shear, base moment, inter-story drift and story displacement. Furthermore, to obtain the crack patterns and the ductility of the walls, static inelastic analyses were carried out using accurate finite element models. The results reveal that despite a small reduction in the strength of shear walls with openings, the crack patterns distribute more uniformly, and the ductility increases as the opening becomes larger.

1. Introduction

Shear walls have long been recognized in medium height buildings as lateral load resisting systems. This is due, mostly, to their ability in providing the required level of lateral stiffness and strength for the structure. Despite their names, shear walls are usually considered as large-scale cantilever beams with dominated bending behavior. This viewpoint is apparent in design codes where all steps are taken to ensure the ductility of shear walls by preventing their shear mode of behavior as a brittle mode. The comparison of the behavior factors manifests that the behavior factor of special steel moment frames is much greater than that of special reinforced concrete shear walls. Beside other lateral load resisting systems, it can be deduced that shear wall has not been presented as a ductile system. Nevertheless, various methods have been proposed to improve the ductility of shear walls [1]. On the other hand, from

an architectural point of view, ordinary shear walls are almost recognized as a restricted element for the interior design of a structure.

Since the maximum flexural moment and subsequently the maximum curvature in shear walls due to earthquake loads happens at the base of the wall, it is expected that the flexural hinge forms at this area, see Figure (1). According to this figure, it is obvious that the plastic hinge happens only in a small region at the base of the wall (i.e. L_P) where the input energy of lateral loads dissipates. In this ductility mode, upper parts of the wall are subjected to rigid body movement due to the plastic curvature at the bottom of the wall. Consequently, the ductility resource of the rest of the wall is not engaged in the response of the structure.

It should be noted that the formation of plastic hinge at the base of the wall might cause serious
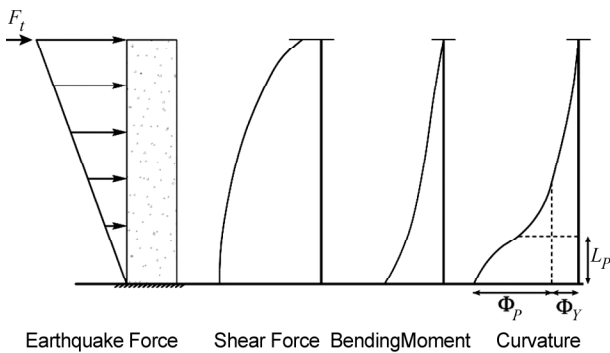
Figure 1. The schematic static response of a shear wall due to earthquake loads.

problems for the vertical load carrying capacity.

Experimental tests show that the plastic hinge, where the most inelastic deformations occur, spreads across the distance equal to the width of the wall. The ductility of this area depends directly to the reinforcement details [3]. Early tests of isolated walls under static monotonic and cyclic reversed loading have indicated that the concentration of well-confined longitudinal reinforcement at the end of a wall section can significantly increase the ductility of the wall [4-6].

The system performance can improve by distributing the energy dissipation across the wall-height. This can be addressed by preventing the dominance of flexural failure mode and limiting the inter-story drifts.

In order to enhance the ability of shear walls in dissipating the input energy, several solutions can be given. One of the impractical solutions is reducing the flexural strength across the height of the wall to spread the plastic flexural mechanism. Considering the minimum reinforcement requirements in the wall, it can be possible only by decreasing the width of the wall proportion to the rate of bending moment reduction. Another solution for improving the behavior of *RC* shear walls is to propagate the shear mechanism along the height of the wall by reducing the wall thickness. The shear area of the wall is calculated so that the inter-story drift reaches its allowable value under the story shear force. In this case, the boundary elements at both ends of the wall provide the flexural strength. As a result, the required thickness of the wall to be set to achieve the ultimate shear inter-story drift is inaccessible [7].

As shown in the Figure (1), bending moment reduced rapidly along the height of the wall and left

limited room for energy absorption potential in the wall system. Shear force, however, is distributed more uniformly across the height. Considering the special distribution of internal forces, energy dissipation can be occurred not only at the base flexural plastic hinge with large bending moment, but also at the upper part of the wall using shear mechanism where bending moment is small enough versus shear force. Therefore, two distinct energy absorption mechanisms can be utilized in both flexural and shear mode. According to random distribution of seismic loads along the height of the wall, the probability of energy dissipation is provided in both mechanisms simultaneously or even separately. In addition, trilinear behavior of reinforced concrete has the significant role in providing the foundation of development of plastic flexural and shear hinges. Therefore, using shear and flexural ductility modes results in a Dual Ductility mode Shear Wall (*DDSW*).

According to the previous discussion, it is deduced that the conventional shear wall cannot provide both ductility modes together. To this aim, this concept can be extended to the shear walls with openings. Several aspects for such a system as well as coupled and slit shear walls are illustrated in Figure (2) [8].
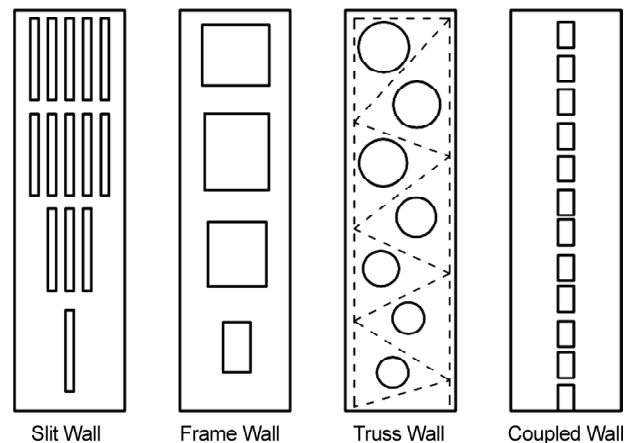

Figure 2. Sample layouts of dual ductility mode shear walls, after Ziyaeifar [6].

The position and characteristics of opening should be selected regarding the interaction of shear force and bending moment. Accordingly, due to large bending moment at the base of the wall and the destructive effect of shear force on flexural capacity, the shear strength of the wall section at this region should be large enough to avoid any shear

failure. Therefore, any openings should not be utilized at the base of the wall. Whereas, in upper part of the wall, because of large reduction in bending moment compared to shear force, their interaction is low and the energy dissipation can be employed in shear mechanism. In order to better use of shear ductility mode over the wall height, it is necessary to enlarge the opening dimension proportionate to reduction of shear force along the height.

Appropriate distribution of openings in the wall can easily lead to improve the classic criteria of these walls, such as the dynamic characteristics, nonlinear behavior, and the ductility of the structure. Moreover, using openings in the shear walls may be acceptable as interior design and architectural point of view.

As mentioned, one of the most well known shear walls with openings is the Coupled Shear Wall (*CSW*). In many structural walls, a regular pattern of openings will be required for architectural purpose. *CSWs* are a form of construction often used in moderately high multi-story reinforced concrete buildings. Using openings in a regular and rational arrangement leads to efficient structural systems, particularly suited for ductile response with very good energy dissipation characteristics. The main reason for this implication is that the connecting beams are considerably weaker than the walls and have the ability to dissipate the energy if detailed properly [2, 9]. Actually, special complex reinforcement details are required to provide high local ductility demands in connecting beams. Several theoretical and experimental researches have been devoted to evaluate the behavior of coupled shear walls [10-15]. However, Paulay [16-17] carried out a noticeable research that has a considerable contribution to the understanding of hysteretic behavior of *CSW* systems and the ability of such walls in distributing the inelastic behavior along the height of the wall.

Furthermore, having the ability in dissipating the energy along the height of the wall, *RC* slit shear walls can be also categorized as lateral load resisting systems. To study the behavior of slit shear walls, various experimental and theoretical investigations have been conducted. The results indicate that yielding of the connecting beams could considerably reduce the lateral displacement and enhance the behavior of slit shear walls [18-22].

It should be noted that failure mechanism of coupled and slit shear walls occurred as plastic hinges formed at link beams ends together with the base of the wall. This is, however, in contradiction with the concept of dual ductility, which can provide a situation for using any of the ductility modes even separately.

In order to study the role of openings in ductile behavior of shear walls, it is aimed at investigating the inelastic dynamic and static behavior of *DDSWs*. In this regard, a series of dynamic analyses was performed to understand the general dynamic behavior of these walls. In this case, a simple two-dimensional (*2D*) model was used to idealize the shear walls. Moreover, to be able to compare the crack patterns and ductility enhancement of such walls with conventional shear walls, various static inelastic analyses were carried on some finite element models of *DDSWs*.

2. Dynamic Nonlinear Analysis of Dual Ductility Mode Shear Walls

In order to investigate the energy dissipation potential of the *DDSW*, it is necessary to perform dynamic analysis. However, static analysis cannot be employed to describe the behavior of the system with dual plastic hinges [23]. To this aim, a shear wall with varied opening along the height is considered. In this section, some numerical results are provided to assess the capability of *DDSW* in dissipating the input energy under seismic loads, especially in shear mode along the wall height.

The fundamental difference between *CSW* and this kind of *DDSW* is the way of distributing the plastic behavior along the height of the wall. Generally, *CSW* is designed in a way that their behavior becomes similar to the moment frames, and the plastic hinges form at all the link beams before ultimate failure mechanism. Therefore, to avoid undesirable failure and provide sufficient ductility, complex reinforcement details are required for the beams. Applying the concept of dual ductility for *CSW* (i.e. by changing the dimension of opening along the height of the wall) leads to propagate appropriately the input energy across the height of the wall instead of any concentration only at connecting beams. Accordingly, lower localized ductility demand is required for the link beams and subsequently simpler reinforcement details can be provided in this region.

2.1. Model Manifestation

There are several models for analyzing the shear walls with opening such as *CSWs*. The most common models utilized for analyzing these shear walls are simple truss model, equivalent frame model, continuous model, and finite element model [24-26].

In the equivalent frame method, both the walls and the coupling beams are modeled with frame elements. In this method, it is assumed that the sectional properties are concentrated in the vertical centerline of the cantilever wall. On the other hand, with a simple truss model, the behavior of shear walls with large openings can be approximated easily. It should be noted that truss models are only valid for slender shear walls [27]. In this model, a single module consists of rigid horizontal beams, equal in length to the width of the wall segment, connected to the columns and a diagonal brace. The columns simulate the bending and axial stiffness, while the diagonal braces provide the shear stiffness of the wall. Based on the previous research conducted by authors, the rigid zone at the connections of the element cannot be defined correctly in the equivalent frame approach [28]. Therefore, this approach cannot easily be able to predict the true behavior of the *DDSWs*. Although the finite element models are the most accurate ones for this purpose,

due to the complexity in dynamic analysis of these models, it is decided to employ the simple truss elements in seismic analysis of shear walls using *DRAIN-2DX* program. The elements of the truss model are simple inelastic bar element which can transmit axial load [29].

All the walls considered in this study are assumed as a part of an official building the wall section view of which is presented in Figure (3). It is designed to resist all the combinations of gravity and earthquake loads specified by Iranian Code of Practice for seismic resistant design of buildings [30]. Reinforcement details of the walls are presented in Table (1). Opening dimension and the reinforcement details of coupling beams are shown in Table (2).

Table 1. Reinforcement details of walls.

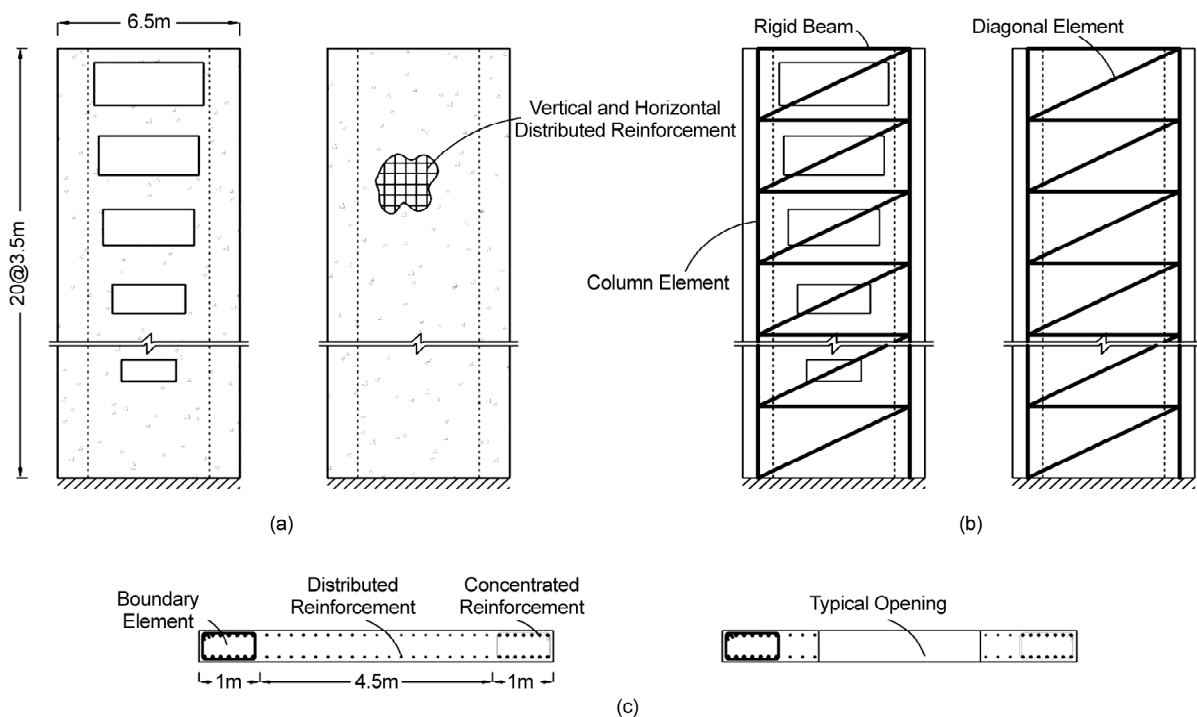| Story	Vertical Rebars		Horizontal Rebars
	Concentrated	Distributed	Distributed
1 to 4	14Φ32	Φ12@300	Φ12@200
5 to 6	8Φ32 + 2Φ25	Φ12@300	Φ12@250
7 to 8	4Φ32 + 4Φ25	Φ12@300	Φ12@250
9 to 12	8Φ25	Φ12@300	Φ12@300
13 to 20	6Φ25	Φ12@300	Φ12@300

Figure 3. Properties of shear walls; (a): Geometric; (b): simple truss model; (c) typical wall section and reinforcement details.

Table 2. Opening dimensions and the reinforcements of the link beams.

Story	Opening Ratio	Opening Dimensions	
		Height	Width
1 to 3	0%	-	-
4 to 5	13%	1250	2400
6 to 7	21%	1600	3000
8 to 9	26%	1800	3300
10 to 11	40%	2200	4100
12 to 15	48%	2450	4500
16 to 20	57%	2650	4900

Bending moment in shear wall can be substituted by coupling axial forces, which are usually, applied to the boundary elements at the end of wall section. Therefore, vertical elements of truss model that simulate the bending effect are considered at the center point of boundary zone of the wall section. Axial stiffness and strength of these elements are calculated based on flexural strength of the wall section, which is converted to a pair of coupling axial force with a specific distance (i.e. the distance between the center points of boundary elements). As mentioned before, the trilinear behavior of reinforced concrete has a significant effect on distributing of plastic hinges over the height of the wall. Therefore, to have a better approximation of the behavior of reinforced concrete elements, column elements are considered to behave based on trilinear behavioral model using specific combination of bar elements.

In order to simpler assessment of the effect of shear mechanism in energy dissipation, only diagonal elements are employed to simulate the shear stiffness of the wall, while horizontal bars are considered as rigid elements. The stiffness and strength of the diagonal braces are calculated based on structural analytical relationship, obtained by equating the flexural frame with an equivalent truss model. Accordingly, the shear capacity of the wall section at each level is considered by the strength of these diagonal bars. However, using openings in the middle part of wall section leads to the reducing of the shear stiffness and strength of the wall section. Therefore, any reduction in section area of the diagonal bar, reduce its stiffness and practically can simulate the effect of the opening in the wall. Consequently, using this simple truss model can easily provide us an operational competent tool for assessment of the potential of energy dissipation due to shear force.

It should be noted that the *OSW* and *DDSW* models considered in this research have the same flexural stiffness, which is provided by boundary elements at both ends of the wall, but they differ only in their diagonal braces. According to the modal analysis results, the first natural period of the *OSW* and *DDSW* are 2.13 and 2.18 *sec*, respectively.

2.2. Time History Results

To provide better insight into the seismic response of the *DDSW*, extensive inelastic dynamic analyses have been conducted. In this regard, a set of seven earthquake records; Taft, *E*l Centro, Santa Barbara, San Fernando, Tabas, Northridge, and Kobe are utilized as input excitations. All of the earthquake records are scaled to the peak ground acceleration equal to 0.4*g*. To evaluate the seismic inelastic response of *DDSW*, several parameters such as the distribution pattern of the dissipated hysteresis energy across the height of the wall, an introduced energy dissipation index, inter-story drift and story displacement, base shear and base moment are considered.

The comparison between the average values of hysteresis, viscous and total energy dissipated during the analysis shows that the amount of the energy in *OSW* and *DDSW* are very close to each other. The average of hysteresis and viscous energy in the selected earthquakes for *OSW* and *DDSW* are (386 and 399 *kN.m*) and (391 and 397 *kN.m*), respectively.

The distribution pattern of the mean values of hysteresis and viscous energy dissipated across the height of the shear walls under the aforementioned earthquakes is presented in Figure (4).

Although the total hysteresis energy is approximately equal for both *OSW* and *DDSW*, it is indicated that the dissipated energy in *DDSW* distributed more uniformly. Meanwhile, the amount of dissipated energy at the first third floor (i.e. L_p) of the *OSW* is about 70 percent more than that of *DDSW*. Therefore, most of the input energy dissipated at the lower part of *OSW* and subsequently, the damages concentrate at small fraction of the wall. Accordingly, by spreading the dissipated energy across the height, the *DDSW* prevents the accumulation of the damages at special portion of the wall. Thus, the ductility resources of all parts of the wall can be utilized to have a more desirable ductile behavior and subsequently the reinforcement
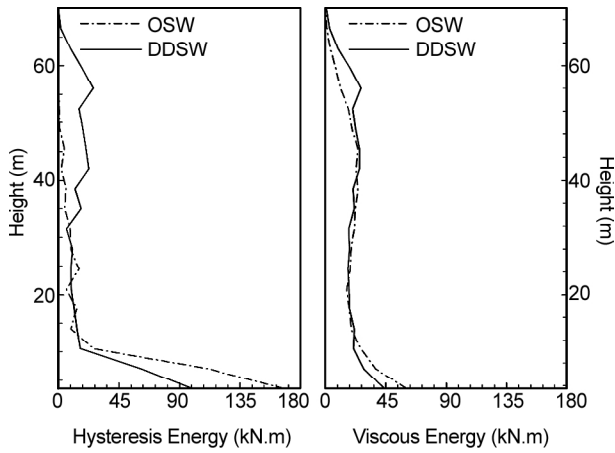
Figure 4. The distribution pattern of the average values of hysteresis and viscous energy in OSW and DDSW across the height of the wall under the earthquakes.

details and confinement requirements at the base of the wall would become more simplified.

One way of numerically quantifying the seismic damage suffered by buildings is by making use of damage indices. Among the many damage indicators available, the Park and Ang damage index appears to be the most acceptable due to its simplicity and extensive calibration against experimentally observed seismic damage in reinforced concrete structures [31]. The latest damage index for reinforced concrete building with different types of structural systems introduced by Ghobarah [32] related to the inter-story drift is as follows:

$$SDF = \frac{\sqrt{\frac{1}{(n-1)^2}\sum_{i=1}^{n}(S_i - \overline{S})^2 \sum_{i=1}^{n}(S_i)^2}}{\overline{S}} \quad (1)$$

where *SDF* is the story damage factor and S_i, $\overline{S}$, and *n* are the maximum inter-story drift of floor *i*, the mean value of the maximum inter-story drift ratios, and the number of stories, respectively.

It should be noted that most of these damage indices explain the overall damage of the systems and cannot be able to specify the distribution pattern of the damage along the height of the structures. Moreover, to be able to discuss about the energy dissipation along the height of the wall an energy dissipation index (I_E) is defined as:

$$I_E = \frac{\sum_{i=1}^{n} h_i E_{D_i}}{H_t \sum_{i=1}^{n} E_{D_i}} \quad (2)$$

where h_i, E_{D_i}, H_t and *n* are the height of ith story, total dissipated energy at the same story, total height of the structure and the number of stories, respectively. Higher value for I_z shows that the input energy can be dissipated in a larger extend across the height of the wall. According to Table (3), the mean values of the damage index defined by Ghobarah for *OSW* and *DDSW* are approximately equal. It is concluded that these two types of shear wall have the same damage level. However, the previous results indicate that *OSW* and *DDSW* completely differ in the distribution of the damage (i.e. energy dissipation) along the height of the wall. As a result, the mean values of introduced damage index are 0.27 and 0.41 for *OSW* and *DDSW*, respectively. It is deduced that the inelastic behavior in the *DDSW* spreads in a larger extend along the height of the wall compared to *OSW*.

Table 3. Comparison of introduced damage index with the one suggested by Ghobarah [29].

Earthuakes	Ghobarah Index		Energy Dissipation Index	
	OSW	DDSW	OSW	DDSW
El Centro	0.35	0.36	0.24	0.37
Kobe	0.39	0.42	0.25	0.38
Northridge	0.37	0.43	0.26	0.43
Santa Barbara	0.47	0.52	0.27	0.44
San Fernando	0.45	0.48	0.31	0.43
Tabas	0.46	0.47	0.28	0.41
Taft	0.39	0.46	0.26	0.41
Average	0.41	0.45	0.27	0.41

The average of maximum inter-story drift and story displacement as other damage indexes are illustrated in Figure (5). The figure represents that the inter-story drift of the *DDSW* decreases at most part, especially at the base and top of the wall. Despite the small value for the inter-story drift at the base of the *OSW*, Figure (4) shows that the amount of the energy dissipation in this region is higher than that of the *DDSW*. This is because of the considerable value of the curvature at the base of the *OSW*. Moreover, as shown in Figure (5), the story displacement of the *DDSW* is a little bit smaller than the *OSW*. According to these two figures, it is indicated that both shear and flexural ductility modes are utilized appropriately.

Table (4) presents the comparison of the average

and maximum inter-story drift as well as the top displacement for both *OSW* and *DDSW*. It is shown that the mean value of these parameters for *DDSW* is reduced to about 6.3%, 1%, and 7.6%, respectively. Thus, it is concluded that using openings in the shear walls not only does not weaken the structural system against the seismic loads, but

Figure 5. The mean values of maximum displacement and inter-story drift of OSW and DDSW under the earthquakes.

also improve the performance of these types of the wall and can decrease the local ductility demands.

The base shear and moment of the walls due to the selected earthquakes are presented in Table (5). The results indicate that the average of the base shear and moment induced on *DDSW* decrease to about 15.6% and 3.9%, respectively. Considering this fact that the first natural period of these walls are very close to each other, it can be stated that the reason for the decrease in the response of *DDSW* may be due to its higher damping. Figure (6) shows the time histories of the base shear and moment for *OSW* and *DDSW* under the El Centro earthquake.

In order to predict the ability of the structural systems in energy dissipation, a numerical algorithm is proposed by authors to determine the alternate damping ratio during any excitation according to the energy response of the structure [33]. To this aim, a time-window with a definite width is moved over the whole time history of the dissipated and strain energy. During each time-window, it is assumed that the rate of increase in the dissipated energy is
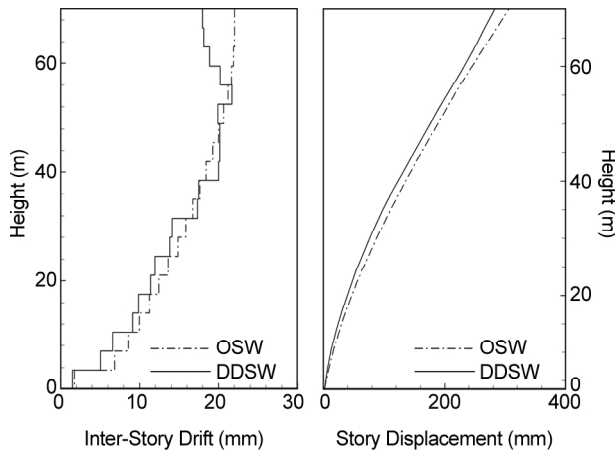
Table 4. The top displacement, the average and maximum inter-story drift of OSW and DDSW under the earthquakes.

Earthquakes	Average Inter-Story Drift (mm)		Maximum Inter-Story Drift (mm)		Top Displacement (mm)	
	OSW	DDSW	OSW	DDSW	OSW	DDSW
El Centro	20.0	17.2	26.8	23.2	386.9	331.8
Kobe	16.3	16.6	22.1	24.5	316.6	321.2
Northridge	17.0	15.8	23.1	22.8	333.5	311.8
Santa Barbara	17.2	16.3	22.9	24.4	333.9	316.8
San Fernando	14.6	12.4	21.5	19.9	266.7	217.3
Tabas	13.6	13.9	19.3	20.3	270.4	273.1
Taft	12.2	11.2	18.6	17.4	227.7	206.6
Average	15.8	14.8	22.0	21.8	305.8	282.7

Table 5. The base shear and moment of OSW and DDSW under the selected earthquakes.

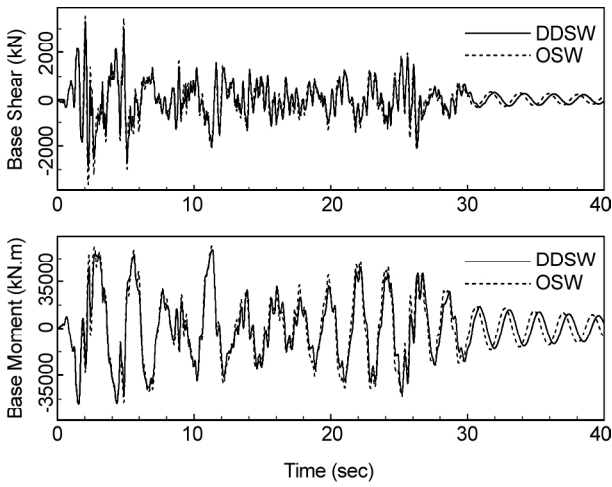| Earthquakes	OSW		DDSW	
	Base Shear (kN)	Base Moment (kN.m)	Base Shear (kN)	Base Moment (kN.m)
El Centro	3619	62073	3271	59230
Kobe	3465	57298	2980	54812
Northridge	3540	56252	3043	54525
Santa Barbara	2770	60690	2620	58241
San Fernando	2645	56496	2494	53207
Tabas	2780	53394	1910	53571
Taft	3384	58042	2425	54959
Average	3172	57749	2678	55506

Figure 6. The time histories of base shear and base moment for OSW and DDSW under the El Centro earthquake.

constant, and the strain energy can be extracted as the average value. Thus, to calculate the dissipated energy, the difference between the amount of energy at the beginning and the end of the window with the width of T is required, while for the strain energy, the average amount of energy at both ends of the window should be obtained.

In general, the damping coefficient of a system is given by a dimensionless damping ratio as [32]

$$\xi = \frac{c}{c_{cr}} = \frac{c}{2m\omega_n} \qquad (3)$$

where m, c, c_{cr}, and ω_n are the mass, damping coefficient, the critical damping value, and the fundamental frequency of the system, respectively.

Considering the damping as a parameter which specifies the potential of energy dissipation, the damping ratio can be calculated from the equilibrium of energy in the system. The total input energy E_I, the structure is exposed to since the beginning of the excitation can be decomposed as follows [34]:

$$E_I = E_K + E_D + E_S + E_Y \qquad (4)$$

in which E_K is the relative kinetic energy of the mass, E_D is the dissipated energy due to viscous damping, E_S is the recoverable strain energy and E_Y is the energy dissipated by yielding.

Generally, the Equivalent Viscous Damping (*EVD*) ratio ξ_{eq} is calculated based on equating the energy dissipated in each cycle of vibration of a real structure to a Single Degree of Freedom (*SDOF*) system. In the steady-state vibration of a *SDOF* system under a sinusoid external force as

$p = p_0 \sin(\overline{\omega}t)$, the value of ξ_{eq} is derived as [32]

$$\xi_{eq} = \frac{\omega_n}{4\pi\overline{\omega}} \cdot \frac{E_{D_0}}{E_{S_0}} \qquad (5)$$

in which E_{D_0} and E_{S_0} are the dissipated energy and strain energy in one cycle of the excitation, respectively.

Eq. (5) gives an expression for evaluation of *EVD* ratio when the structure is under a harmonic excitation with a specific frequency. For real structures, which are generally exposed to random loads with wide frequency content, Eq. (5) is not capable of describing the equivalent damping ratio. However, the most contribution of the natural modes in the dynamic response of a structure and consequently, the energy dissipation occurs when the excitation frequency is in the vicinity of the natural frequencies. In order to resolve this problem, we use the following relation for evaluation of *EVD* ratio

$$\xi_{eq} = \frac{E_{D_0}}{4\pi E_{S_0}} \qquad (6)$$

Actually, Eq. (6) is the same as Eq. (5) when $\overline{\omega} = \omega_n$. According to Figure (7), within any window,
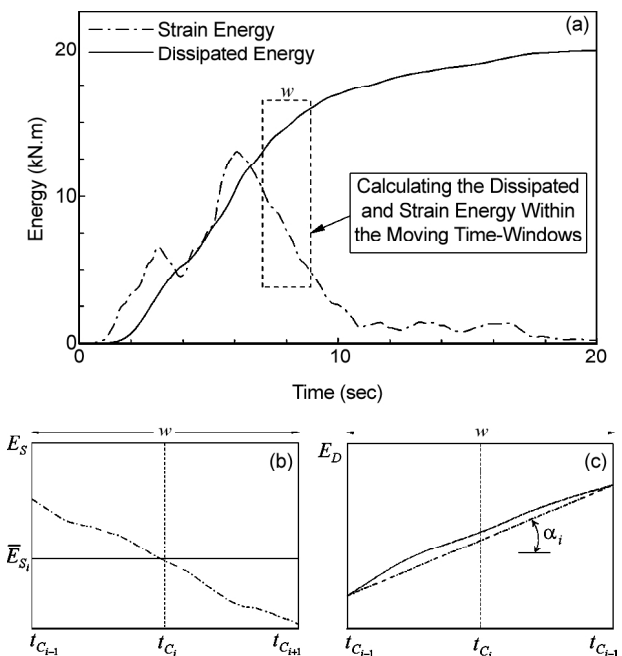

Figure 7. The schematic procedure for Calculating the introduced damping ratio based on the proposed algorithm. (a) Typical time history of the dissipated and strain energy swept by a moving time-window. (b) The strain energy in a considered time-window. (c) The dissipated energy in a considered time-window.

the dissipated and average of strain energy, $\overline{E}_{D_i}$ and $\overline{E}_{S_i}$ at time $t_{C_{i+1}}$ can be stated as

$$\overline{E}_{D_i} = \alpha_i T; \quad \overline{E}_{S_i} = \frac{E_{S_{i+1}} + E_{S_{i-1}}}{2} \quad (7)$$

Where

$$\alpha_i = \frac{E_{D_{i+1}} - E_{D_{i-1}}}{\omega} \quad (8)$$

and $E_{D_{i-1}}$, $E_{D_{i+1}}$, and $E_{S_{i-1}}$, $E_{S_{i+1}}$ are respectively the dissipated and strain energy at the beginning and the end of the window (i.e. at the time of $t_{C_{i-1}}$ and $t_{C_{i+1}}$, respectively). Now, using Eq. (6) along with Eq. (7) and (8) at each instant, gives the value of ξ_{eq}.

As a result, the comparison between the alternate damping ratio for hysteric behavior in *DDSW* and *OSW* under the El Centro earthquake is shown in Figure (8). It is indicated that the proposed damping ratio is higher in most part of the time history, which is an important change in dynamic characteristics of these types of the shear walls. The average of the proposed damping ratio for *DDSW* is increased to about 20%. Consequently, a design spectrum with higher damping ratio can be recommended for seismic design of the *DDSWs*.
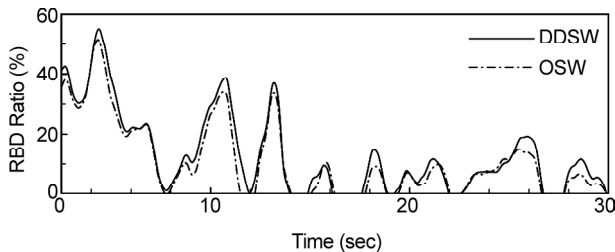

Figure 8. The alternate damping ratio for DDSW and OSW under the El Centro earthquake.

Based on the above-mentioned results and discussions, it is expected that the *DDSWs* can be designed for a smaller base shear than the conventional shear wall. Subsequently, simpler detailing for reinforcement can be used for the whole structure. The seismic responses of the both shear walls under the selected earthquakes point out that the concept of dual ductility mode shear walls can be applied with simplicity for the conventional shear walls.

3. Static Nonlinear Analysis of Dual Ductility Mode Shear Walls

To provide better insight into the behavior of such

walls, extensive inelastic analyses using finite element models are needed. Being time-consuming and complex, it is preferred to perform static inelastic analysis rather than dynamic analysis. Therefore, it is possible to evaluate the crack pattern and verify the ductility modes of shear walls with openings. In this regard, this method is utilized to analyze the shear walls with slits (*SSW*) as another type of the *DDSWs* using general-purpose *FE* program, *TNO DIANA* [35].

3.1. Model Manifestation

In order to comprehensive understanding of the role of openings in the ductility characteristics of shear walls, three types of fixed base shear walls-an *OSW*, and two slit shear wall, *SSW*1 and *SSW*2- have been selected. In these *SSWs*, the width of the slits in both *SSWs* is $200\,mm$ and the heights of them are $1000\,mm$ and $2000\,mm$, respectively. All the walls have $24\,m$ height, $6\,m$ width with the thickness of $300\,mm$. The reinforcement ratio (i.e. the ratio of the area of total reinforcement to the nominal section area of the wall) in the central part of the wall and the boundary zones are 1% and 2%, respectively. To study the static nonlinear behavior of *DDSWs*, a series of pushover analyses under cumulative triangular distributed loads has been performed on the selected shear walls [36].

The specimens are modeled with eight-node brick elements and the governing nonlinear phenomena in the ultimate limit state are cracking and crushing of concrete and plastic behavior of reinforcement steel using displacement control approach. The behavior of concrete is idealized using modified Maekawa model, which combines a multi-axial damage plasticity model for the effect of crushing in the compressive behavior with a crack model based on total strain for the tensile part of the behavioral curve, considering the strength deterioration of cracked concrete. Besides, the model describes hysteretic behavior in tensile and compressive unloading-reloading loops. The constitutive behavior of the reinforcement steel was modeled by Von-Mises plasticity model with isotropic strain hardening. The equivalent thickness method is used for the reinforcement bars in both directions. The material properties used in this research are summarized in Table (6) and Figure (9). The graphs are depicted based on the governed relationship presented for material models.
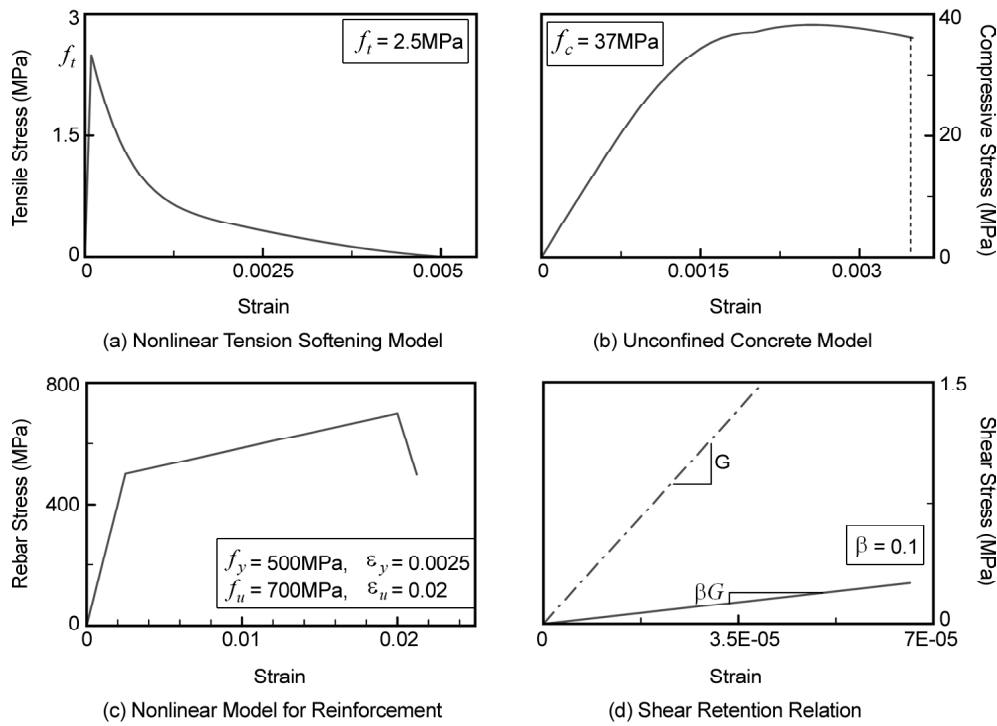
Figure 9. Nonlinear material models for Concrete and reinforcement bars.

Table 6. A summary of material properties for finite element models.

Material		Characteristic	
Concrete	Compression	Poisson's Ratio	0.2
		Density	2400kg/m³
		Compressive Strength	37MPa
		Young's Modulus	28000Mpa
	Tension	Fracture Energy	0.24N/mm
		Crack Band Width	100mm
		Tensile Strength	2.5MPa
Steel	Tension	Young's Modulus	200000MPa
		Yield Strength	500MPa
		Ultimate Strength	700MPa

To achieve equilibrium at the end of the increment, an iterative solution algorithm, Quasi-Newton method (also called 'Secant method') is used. The Quasi-Newton methods implemented in *TNO DIANA* are known as the Broyden, the Broyden-Fletcher-Goldfarb-Shanno (*BFGS*) and the Crisfield methods, the last of which is applied in this research. To attain a good convergence, the energy norm, which is composed of internal forces not the out-of-balance force and relative displacements, is employed in this analysis [35].

3.2. Numerical Results

The patterns of large cracks in shear walls under static incremental lateral load are shown in Figure (10). The concentration of these considerable cracks and subsequently, the significant damages at the lower part of the *OSW* indicates that most part of the wall does not contribute in the energy dissipation procedure during lateral loading. It is while, in the *DDSWs* (i.e. *SSW*1 and *SSW*2), the cracks propagate in link beams along the height of the wall. Therefore, the damages induced by the lateral loads spread across the height of the *DDSWs* without any localization at any particular region and consequently, the local ductility demand will be decreased.

Figure (11) illustrates the pushover curves for the aforementioned walls. Despite a small decreasing in the strength and stiffness of the *DDSWs*, it is deduced that using some openings such as regular slits in the shear wall improve the ductility of the wall. The comparison between the results of pushover and dynamic analysis shows that the amounts of maximum top displacement of the walls are considerably different. According to Krawinkler and Seneviratna [37] and Tso and Moghadam [38] the pushover method is rarely used to predict the seismic demands. Notwithstanding, if this method is utilized as a tool for predicting seismic demands instead of estimating capacities, the analysis is usually performed
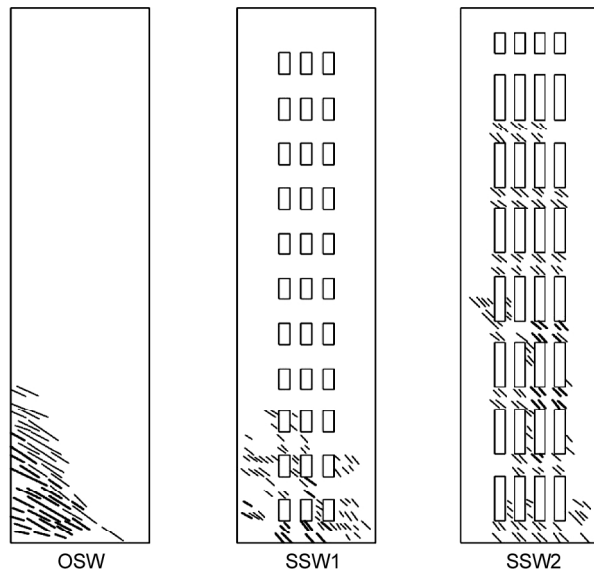
Figure 10. Significant large cracks in OSW, SSW1, and SSW2 under nonlinear incremental static analysis.
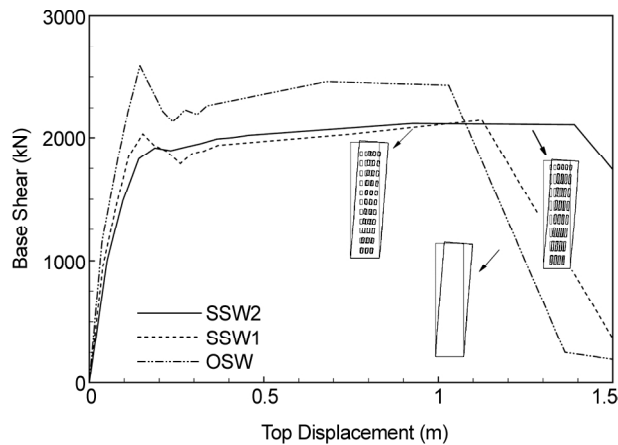

Figure 11. The pushover curves for OSW, SSW1, and SSW2.

until the roof displacement corresponding to the design ground acceleration is attained. Clearly, the top displacement in this case is not only smaller than the ultimate value obtained in pushover analysis, but also it is usually beyond the global yield limit states [39].

4. Conclusion

Commonly used analytical models, simple truss, and finite element models were utilized in a non-linear static and dynamic analysis to investigate the behavior of shear walls with opening considered as dual ductility mode shear walls. Findings projected from this investigation provide better insight into ductile behavioral aspects of these walls. The results of inelastic dynamic analysis on a variety of shear

walls indicate that rational arrangement of openings can improve the dynamic characteristics and nonlinear behavior. As a result, the amount of the dissipated energy for the first fourth floor of these types of the wall is decreased to about half the value for ordinary shear walls. However, the energy dissipation dispersed across the height of the wall without any concentration of damages at the base of the wall. Consequently, local ductility demands in this region will decrease and subsequently simple detailing for reinforcement are required. In addition, the response of these types of the wall such as base shear, base moment, top story displacement, and average value of inter-story drift along the height are reduced to about 15.6%, 3.9%, 7.6%, and 6.3%, respectively. Furthermore, the results of inelastic static analysis demonstrate that despite the small reduction in strength and stiffness of the wall, the openings can improve the ductility of these walls by propagating the large cracks in a more extensive region along the height of the wall. According to the results of this work, it can be said that these types of the wall provide better structural behavior beside their suitable architectural aspects.

References

1. Omori, N., Takahashi, T., Tanaka, H., and Watanabe, S. (1976). "Studies on the Reinforced Concrete Slitted Shear Walls", Ph.D. Dissertation, Department of Civil Engineering, University of Tokyo, Japan.

2. Paulay, T. and Priestley, M.J.N. (1992). "Seismic Design of Reinforced Concrete and Masonry Buildings", New York, US, John Wiley and Sons.

3. Oesterle, R.R., Fiorato, A.E., and Corley, W.G. (1980). "Reinforcement Details for Earthquake-Resistant Structural Walls", ACI Concrete mt, 55-66.

4. Cardenas, A. and Magura, D.D. (1973). "Strength of High-Rise Shear Walls-Rectangular Cross Section. In: Response of Multistory Concrete Structures to Lateral Forces", ACI Publication SP-36, American Concrete Institute, Detroit, MI.

5. Oesterle, R.G., Fiorato, A.E., Johal, L.S., Carpenter, J.E., Russell, H.G., and Corley, W.G. (1976). "Earthquake-Resistant Structural Walls-

Tests of Isolated Walls", Report to the National Science Foundation, Portland Cement Association.

6. Oesterle, R.G., Aristizabal-Ochoa, J.D., Fiorato, A.E., Russell, H.G., and Corley, W.G. (1979). "Earthquake Resistant Structural Walls-Tests of Isolated Walls-Phase II", Report to the National Science Foundation, Portland Cement Association.

7. Ziyaeifar, M. (2003). "The Study of the Seismic Behavior of Shear Walls with Dual Ductility Behavior", IIEES Report, International Institute of Earthquake Engineering and Seismology, Tehran, Iran (in Farsi).

8. Ziyaeifar, M. (2001). "Current R&D on Passive Energy Dissipation and Seismic Isolation Techniques in Iran", *7th International Seminar on Seismic Isolation, Passive Energy Dissipation and Active Control of Vibration of Structures*, Italy, 371-377.

9. Chaallal, O. and Chlamallah, N. (1996). "Seismic Response of Flexibly Supported Coupled Shear Walls", *Journal of Structural Engineering, ASCE*, **122**(10), 1187-1197.

10. Schnobrich, W.C. (1977). "Behaviour of RC Structures Predicted by Finite Element Method", *Computers & Structures*, **7**(3), 365-376.

11. Fintel, M. and Ghosh, S.K. (1981). "Application of Inelastic Response History Analysis in the Seismic Design of a 31-Story Frame-Wall Building", *Earthquake Engineering & Structural Dynamics*, **9**, 543-556.

12. Wight, J.K. (1988). "Earthquake Design Compared to Measured Response", *Journal of Structural Engineering, ASCE*, **112**(1), 149-164.

13. Agrawal, A.B., Jaeger, L.G., and Mufti, A.A. (1981). "Response of RC Shear Wall under Ground Motions", *Journal of Structural Division, ASCE*, **107**(2), 395-411.

14. Subedi, N.K. (1991). "RC Coupled Shear wall Structures II: Ultimate Strength Calculations", *Journal of Structural Engineering, ASCE*, **117**(3), 681-698.

15. Chaallal, O. (1992). "Finite Element Model for Seismic RC Coupled Walls Having Slender Coupling Beams", *Journal of Structural*

Engineering, ASCE, **118**(10), 2936-2943.

16. Paulay, T. (1971). "Simulated Seismic Loading of Spandrel Beams", *Journal of Structural Division, ASCE*, (ST9), 2407-2419.

17. Paulay, T. (1971). "Coupling Beams of Reinforced Concrete Shear Walls", *Journal of Structural Division, ASCE*, **97**(ST3), 843-862.

18. Mutoh, K. (1973). "A Study on Reinforced Concrete Silted Shear Walls for High-Rise Building", *5th World Conference on Earthquake Engineering*, Rome.

19. Kwan, A.K.H., Lu, X., and Cheung, Y.K. (1993). "Elastic Analysis of Slit Shear Walls", *International Journal of Structures*, **13**(2), 75-92.

20. Lu, X. and Wu, X. (2000). "Study on a New Shear Wall System with Shaking Table Test and Finite Element Analysis", *Earthquake Engineering & Structural Dynamics*, **29**(10), 1425-1440.

21. Kwan, A.K.H., Tian, Q.L., and Cheung, Y.K. (1998). "Stochastic Response Analysis of Visco-Elastic Slit Shear Walls", *Structural Engineering and Mechanics*, **6**(4), 377-394.

22. Kwan, A.K.H, Dai, H., and Cheung Y.K. (1999). "Non-Linear Seismic Response of Reinforced Concrete Slit Shear Walls", *Journal of Sound and Vibration*, **226**(4), 701-718.

23. Panagiotou, M. and Restrepo, J.I. (2009). "Dual-Plastic Hinge Design Concept for Reducing Higher-Mode Effects on High-Rise Cantilever Wall Buildings", *Earthquake Engineering & Structural Dynamics*, **38**(12), 1359-1380.

24. Santhakumar, A.R. and Paulay, T. (1974). "Ductility of Coupled Shear Walls", Ph.D. Dissertation, Department of Civil Engineering, University of Canterbury, Christchurch, New Zealand.

25. Stafford Smith, B. and Girgis, A. (1984). "Simple Analogous Frames for Shear Wall Analysis", *Journal of Structural Engineering, ASCE*, **110**(11), 2655-2666.

26. Chan, H.C. and Cheung, Y.K. (1979). "Analysis of Shear Walls Using Higher Order Elements", *Building and Environment*, **14**, 217-224.

27. Rombach, G.A. (2004). "Finite Element Design of Concrete Structures", UK, Thomas Telford, Ltd, ISBN: 0727732749.

28. Labafzadeh, M.S.R. and Ziyaeifar, M. (2008). "Seismic Behavior of RC Dual Ductility Mode Shear Walls", *14th World Conference on Earthquake Engineering*, Innovation Practice Safety, China.

29. Parakash, V., Powel, G.H., and Campbell, S. (1993). "DRAIN-2DX Base Program Description and User Gguide", *Earthquake Engineering Research Center*, Berkley, US, University of California.

30. Standard No. 2800. (2005). "Iranian Code of Practice for Seismic Resistance Design of Buildings", Third Edition, Building and Housing Research Center (in Farsi).

31. Park, Y.J., Ang, A.H.S., and Wen, Y.K. (1987). "Damage-Limiting Aseismic Design of Buildings", *Earthquake Spectra*, **3**(1), 1-26.

32. Ghobarah, A. (2004). "On Drift Limits Associated with Different Damage Levels", *Int. Workshop on Performance-Based Seismic Design*, Dept. of Civil Engineering, McMaster Univ.

33. Labafzadeh, M.S.R. and Ziyaeifar, M. (2011). "An Alternate Approach for Evaluation of Energy Dissipation Potential", Submitted.

34. Chopra, A.K. (1995). "Dynamics of Structures Theory and Applications to Earthquake Engineering", New Jersey, Prentice-Hall, ISBN: 8120321391.

35. Witte, F.C. and Kikstra, W.P. (2007). "DIANA-Finite Element Analysis; User's Manual Release 9.2", TNO Building and Construction Research, The Netherlands.

36. Labafzadeh, M.S.R. and Ziyaeifar, M. (2008). "Nonlinear Behavior of RC Dual Ductility Mode Shear Walls", *AIP Conference Proc. Seismic Engineering*, Italy, 1020, 1854-1862.

37. Krawinkler, H. and Seneviratna, G.D.P.K. (1998). "Pros and Cons of a Pushover Analysis of Seismic Performance Evaluation", *Engineering Structures*, **20**(4-6), 452-464.

38. Tso, W.K. and Moghadam, A.S. (1998). "Pushover Procedure for Seismic Aalysis of Buildings", *Progress in Structural Engineering and Materials*, **1**(3), 337-344.

39. Mwafy, A.M. and Elnashai, A.S. (2001). "Static Pushover Versus Dynamic Collapse Analysis of RC Buildings", *Engineering Structures*, **23**, 407-424.